Spectrochimica Acta Part A: Molecular and Biomolecular Spectroscopy 229 (2020) 117877

Contents lists available at ScienceDirect

Spectrochimica Acta Part A: Molecular and Biomolecular Spectroscopy

journal homepage: www.elsevier.com/locate/saa

Advanced direct method to quantify the kinetics of acetohydroxamic acid (AHA) by Raman spectroscopy

Iván Sánchez-García [a,b], Laura J. Bonales [a,*], Hitos Galán [a], Jose Manuel Perlado [b], Joaquín Cobos [a]

[a] Centro de Investigaciones Energéticas, Medioambientales y Tecnológicas (CIEMAT), Avda. Complutense 40, 28040 Madrid, Spain
[b] Instituto Fusión Nuclear, Universidad Politécnica de Madrid (UPM), 28006 Madrid, Spain

ARTICLE INFO

Article history:
Received 16 September 2019
Received in revised form 28 November 2019
Accepted 28 November 2019
Available online 02 December 2019

ABSTRACT

The ligand acetohydroxamic acid (AHA) suffers hydrolysis at acidic conditions. This reaction has been studied for a long time, due to its implications in different applications, by using indirect colorimetric methods. This work shows how Raman spectroscopy can be very useful as a direct technique for measuring the hydrolysis kinetics of AHA, faster, more versatile and easier compared with the indirect traditional UV–Vis method which needs a complex formation with Fe.

Thereby, we present a detailed study of the qualitative and quantitative Raman spectra of 1 mol/L AHA and its hydrolysis products. These results enabled us to perform a complete kinetic study of this molecule at different pH ranging from 0.5 mol/L to 4 mol/L HNO_3, *i.e.* not only at excess acidic conditions but also at limiting nitric acid conditions.

© 2019 Published by Elsevier B.V.

1. Introduction

Hydroxamic acid, with general formula RC(O)NHR´, is an organic weak acid which constitutes one of the most important families of organic ligands for metal complexation. Due to its metal chelating and hydrogen bonding properties, this type of ligand has multiple pharmaceutical applications such as developing drugs against cancer, cardiovascular disease, HIV, and it has also been studied as potential insecticide, antimicrobial and/or corrosive agent [1].

In the nuclear field context, it is widely recognized that hydroxamic acids, like acetohydroxamic acid ($CH_3CONHOH$), can be used in some reprocessing strategies under development of the spent nuclear fuel, such as in UREX (URanium EXtraction) [2]. This process is a modification of PUREX process (Plutonium Uranium Recovery Extraction) [3], to prevent the plutonium co-extraction, where the addition of acetohydroxamic acid, also known as AHA, plays a key role [4,5], due not only to its mentioned chelating capacity but also to its capacity for reducing a selective range of tetravalent and hexavalent ions, such as Pu(IV) and Np(VI) [6–8].

In addition to the AHA capacity for reduction and complexation, it is well known that AHA undergoes hydrolysis at the acidic medium typically used in this process, leading to acetic acid (AcOH) and hydroxylamine (HA), which must be monitored during reprocessing applications [7].

The AHA hydrolysis has been studied at different conditions (AHA concentrations and pH) by several authors [9–15] using indirect measurements. Thus, AHA concentration as a function of time is obtained by the analysis of UV–visible spectrophotometric measurements of AHA bound to ion Fe(III). The Fe(III)–AHA complex exhibits three complexes at AHA:Fe ratios of 1:1, 2:1, 3:1. All three are colored complexes and the corresponding λ_{max} are 498, 460 and 440 nm, respectively [11]. Accordingly, an aliquot of AHA was periodically removed from AHA solution and mixed with $Fe(NO_3)_3$ solution in order to form the Fe(III)-complex [14].

In this paper we take advantage of Raman spectroscopy for measuring the kinetics of AHA hydrolysis. Since Raman spectroscopy allows us to measure concentrations and speciation of several components without any special metal-ligand complexation (M-L) or additional preparation of the sample, this technique can be used for *in situ* measurements [16] *versus* UV-VIS technique, which requires the formation of the colored complex Fe(III)-AHA, and is a time-consuming method. Moreover, Raman technique can be used not only for monitoring the AHA concentration but also the concentration of its hydrolysis products, AcOH and HA.

In order to measure the acidic AHA hydrolysis by Raman spectroscopy, it is necessary to perform the Raman bands assignment and the calibration curves of each molecule involved in the reaction, *i.e.* acetic acid (AcOH) and hydroxylamine (HA).

Thereby, the work is structured as follows: in Section 2, the materials and methods used in this study are described. Then, in Section 3, AHA, AcOH and HA Raman spectra and their assignment are presented and compared with the assignment made by other authors. A quantitative

* Corresponding author at: CIEMAT, Departamento de Energía, Unidad de Residuos de Alta Actividad, Avda. Complutense 40, 28040 Madrid, Spain.
E-mail address: laura.jimenez@ciemat.es (L.J. Bonales).

https://doi.org/10.1016/j.saa.2019.117877
1386-1425/© 2019 Published by Elsevier B.V.

analysis as a function of time for AHA and its hydrolysis products is shown in Section 3.2. Moreover, in Section 3.3, the kinetics of the reaction at different pH is shown and compared with those obtained by the traditional method using UV–visible spectrophotometric measurements. The conclusions of this work are presented in Section 4.

2. Materials and methods

Acetohydroxamic acid (AHA), acetic acid (AcOH), hydroxylamine (HA) were purchased from Acros (Belgium), Probus (Spain), Merck (Germany), respectively, and were used without further purification. Nitric acid, HNO_3, purchased from VWR Chemical, was purified by using a Quartz sub-boiling distillation system (MLS - Milestone). Milli-Q water samples showed TOC levels below 5–10 ppb and measured resistivities higher than 18 mΩ cm^{-1}.

Raman spectra were acquired by using a Horiba LabRam HR evolution spectrometer (Jobin Yvon Technology). The 532 nm laser beam was focused onto the sample through the 5× objective of an Olympus BX41 microscope. The sample was housed in a home-made cuvette designed in order to measure liquid samples (described in detail elsewhere [17]). The scattered radiation was then collected in backscattering geometry, dispersed using a 1800 grooves/mm holographic grating and recorded by a CCD detector (256 × 1024 pixels), obtaining a resolution better than 0.48 cm^{-1}/pixel. A typical spectrum was obtained within 35 s of acquisition time and 15 accumulations. For the kinetic studies, different experiments were performed in order to ensure the reproducibility, *i.e.* one experiment was carried out by acquiring spectra every 15 min up to 8 h and then at 72 and 144 h, and the second one every 30 min for a period up to 8 h, and then after 24 h.

3. Results

3.1. Raman assignment

Fig. 1 shows the 1 mol/L AHA Raman spectrum and the ones of each hydrolysis products: 0.5 mol/L AcOH and 0.5 mol/L HA, both dissolved in 0.5 mol/L HNO_3. These spectra were acquired to provide useful comparative information for assigning AHA spectrum; *i.e.* that structural features of the molecule, both backbone and the functional groups, produce characteristic and reproducible vibrational bands in the spectrum [18].

Raman bands related to aqueous solution of HNO_3 appear, as expected, in the three spectra and correspond to liquid water and NO_3^- ion. In particular, the broad band at high frequencies (2800–3400 cm^{-1}) corresponds to the OH-bond stretching, ν_s(O—H) [19]; the band at ~1630 cm^{-1} to the OH bending, δ_{bend}(O—H) [19]; the band at ~708 cm^{-1} corresponds to the in plane deformation of the NO_3^-, $\delta_{bend}(NO_3^-)$ [20]; the most intense band located at around 1037 cm^{-1} corresponds to the N—O stretching of the NO_3^- ion, $\nu_s(NO_3^-)$ [21]; and the broad bands at ~1400 cm^{-1} are assigned to the asymmetric stretching bands of the nitrate ion, $\nu_{as}(NO_3^-)$. Moreover, in Fig. 1 a high frequency band can be observed at ~2937 cm^{-1} for AcOH and AHA, which corresponds to the C—H stretching of the methyl group, ν_s(C—H) [22].

Besides, the rest of the bands assignments shown in Fig. 1 were obtained as follows. According to the band assignment of hydroxylamine hydrochloride (NH_3OHCl) reported by Krishnan et al. [23], the most intense band of this molecule (~1004 cm^{-1}) corresponds to the N—O stretching, ν_s(N—O). The same assignment had been done for the band at ~912 cm^{-1} of the solid hydroxylamine by R. Nightingale and E. Wagner at ~921 cm^{-1} [24]. Therefore, we have assigned the band found in this work at ~997 cm^{-1} to the N—O stretching vibration ν_s(N—O).

The assignment of the acetic acid Raman spectrum has been performed on the basis of the results of liquid acetic acid assignment published by M. Haurie et al. [25]. The low frequency bands at 708 and 615 cm^{-1} are assigned to the in plane and out plane bending of the structure CCO, δ_{bend}(CCO) and γ_{twist}(CCO) respectively, the low band at ~449 cm^{-1} to the δ_{bend}(CCO) and the peak at ~881 cm^{-1} is ascribed to the C—C stretching band, ν_s(C—C). The medium intensity band at ~1646 cm^{-1} is attributed to the C═O stretching band, ν_s(C═O).

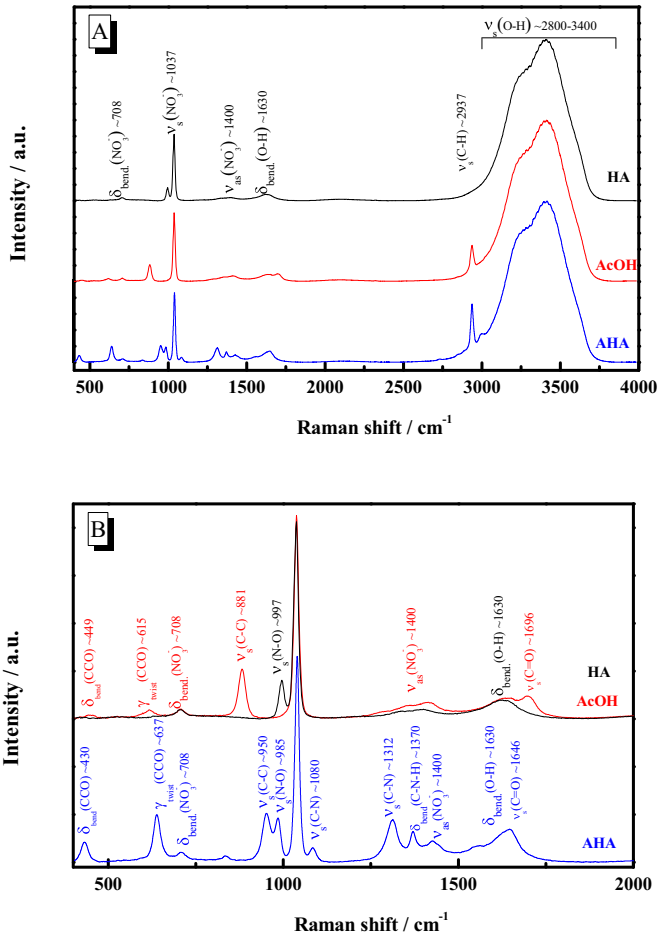

Fig. 1. Raman spectra of 1 mol/L acetohydroxamic acid (AHA), 0.5 mol/L acetic acid (AcOH) and 0.5 mol/L hydroxylamine (HA) dissolved in 0.5 mol/L HNO_3 A) from 450 to 4000 cm^{-1}, and B) from 450 to 2000 cm^{-1}.

The bands assignment of AHA has been deduced by comparison with the assignment of its hydrolysis products. Thereby, we have assigned the bands at ~430 and ~637 cm^{-1} to in plane and out plane bending of the structure CCO, δ_{bend}(CCO) and γ_{twist} (CCO), respectively; bands at ~950 and ~2937 cm^{-1} to the C—C and C—H stretching bands (for acetic acid, ν_s(C—C) = 881 cm^{-1} and ν_s(C—H) = 2937 cm^{-1}); and the band at ~985 cm^{-1} to N—O stretching band (in hydroxylamine ν_s (N—O) = 997 cm^{-1}). Furthermore, as expected, the typical bands of the amide group appear in the AHA spectrum, that is, those related to the C—N and the of C—N—H structure. Hence we have assigned the bands at 1080 cm^{-1}, 1312 and 1370 cm^{-1} to the C—N symmetric stretching and C—N—H in plane bending vibrations, ν_s(C—N) and δ_{bend}(C—N—H).

Scarce publications dealing with the Raman spectra of AHA were found. Holmén et al. [26] had assigned the N—O stretching, ν_s(N—O), to a band around 994 cm^{-1}, which is in agreement with our result, unlike Edwards et al. [27], who assigned the ν_s(N—O) stretch to a band located at ~1091 cm^{-1}. The C═O stretching band, ν_s(C═O), was found at 1642 cm^{-1} by Holmén and at ~1658 cm^{-1} by Edwards, in perfect agreement with our result (1646 cm^{-1}). No other assignments for this

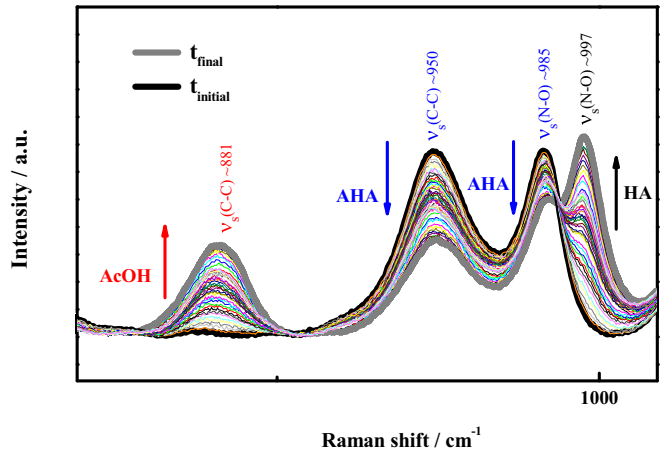

Fig. 2. Raman spectra of 1 mol/L AHA as a function of time (from 0 to 8 h) in 0.5 mol/L HNO_3.

molecule in aqueous solution have been found, but the assignment carried out in this work is in good agreement with the ones shown in other studies related to proteins, such those reported by A. Nevin et al. [28].

3.2. Quantitative Raman spectra analysis

Raman spectroscopy can be used to perform fast, non-destructive and versatile quantitative analysis without sample preparation since the integrated intensity (Area, A) of the Raman scattering is proportional to the concentration (c) [29], as follows,

$$A = (I_L \sigma \eta l)\, c \tag{1}$$

where I_L is the laser intensity, σ is the Raman cross-section or scattering efficiency, η is an instrument parameter and l is the sample path length.

Therefore, if the integrated intensity is normalized with respect to the one corresponding to a constant concentration, *i.e.* an internal calibrant, the following is obtained:

$$A/A_{calibrant} = F/F_{calibrant}\; c/c_{calibrant} \tag{2}$$

where $F_i = (I_L \sigma \eta l)$. Thus, Eq. (1) can be written as a linear equation with a zero intercept,

$$c = a\, A/A_{calibrant} \tag{3}$$

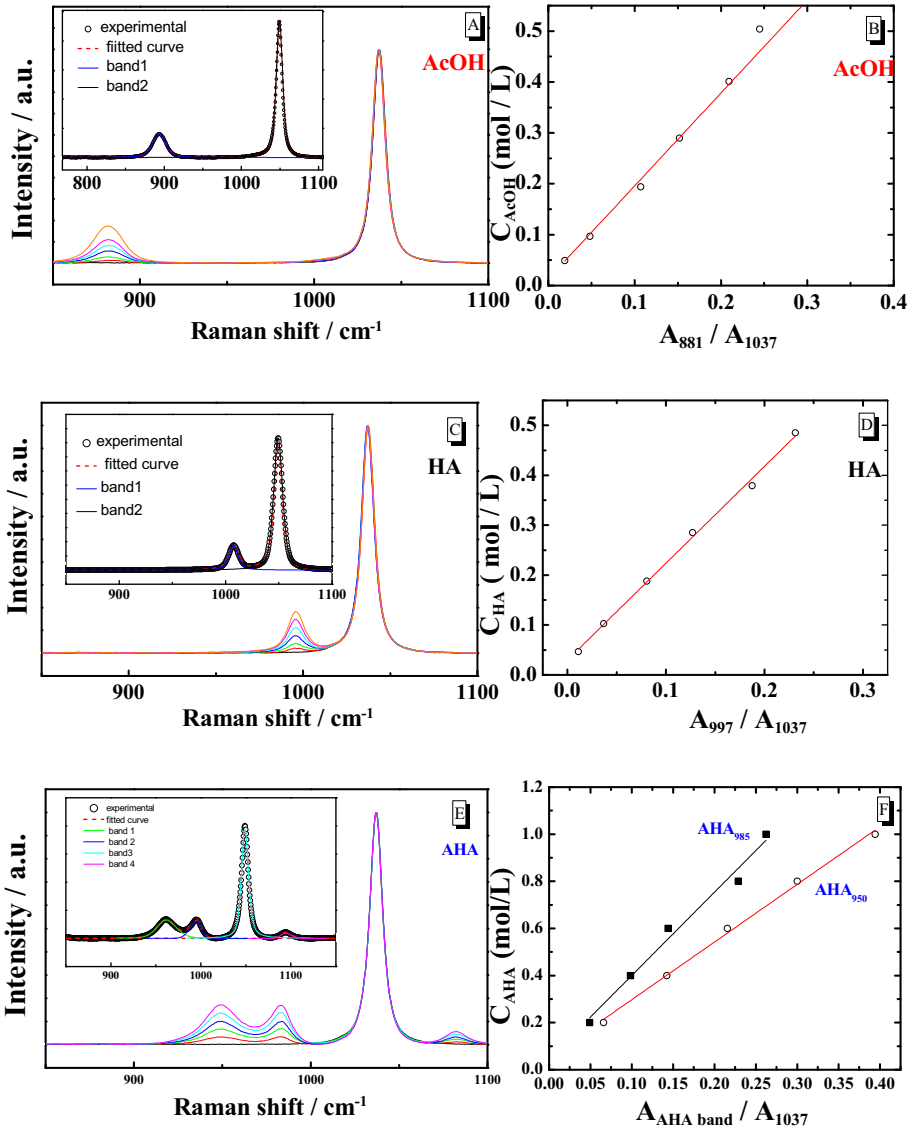

Fig. 3. Experimental Raman spectra, fitted curves and calibration curves corresponding to different concentrations of AcOH (A, B), HA (C, D) and AHA, (D, E), (see text for details).

Table 1
Obtained values of *a* (slope) and *b* (intercept) constants.

Molecule	*a*	*b*
AcOH	1.82 (± 0.05)	0.013 (± 0.009)
HA	1.94 (± 0.05)	0.029 (± 0.007)
AHA	2.45 (± 0.07)	0.05 (± 0.07)

where the slope *a* is defined as $(F_{calibrant} \cdot c_{calibrant})/F$ and can be obtained easily from the plot of a calibration curve of the relative peak areas and the known concentrations.

This feature allows us to study the hydrolysis reaction of AHA as a function of time without the addition of any metal to the solution, which is an advantage for metal complexation applications where AHA is currently involved.

It is well known that AHA hydrolysis is initiated and catalyzed by a hydronium ion, followed by the rate limiting step when the protonated intermediate is attacked by a water molecule [9].

$$CH_3CONHOH\ (aq) + H_3O^+ \rightarrow CH_3COOH + NH_3OH^+ \quad (4)$$

Fig. 2 shows the 1 mol/L AHA spectra obtained every 15 or 30 min for 8 h from 850 to 1030 cm^{-1} in HNO_3 0.5 mol/L.

As it can be appreciated, the intensity of the bands corresponding to AHA (νs(C—C) ~950 and ν_s(N—O) ~985 cm^{-1}) decreases with time, whereas that of the bands corresponding to AcOH (ν_s(C—C) ~881 cm^{-1}) and HA (ν_s(N—O) ~997 cm^{-1}) increase. The concentration of these molecules as a function of time was obtained by using quantitative Raman spectroscopy (QRS). For this purpose, a series of Raman spectra were collected from AHA, AcOH and HA solutions at the following concentrations: 0.05, 0.1, 0.2, 0.3, 0.4 and 0.5 mol/L, for AcOH and HA (Fig. 3.A and Fig. 3.C, respectively); and 0.2, 0.4, 0.6, 0.8 and 1 mol/L for AHA (Fig. 3.E). Note that all spectra were normalized with respect to the integrated intensity of the $\nu_s(NO_3^-)$ band, since it is used as internal calibration.

A band-profile analysis of each spectrum was carried out to track the evolution of the Raman bands as a function of concentration. Second derivative analysis allowed us to obtain the wavenumber of the main contributions, and then a multiple Voigt fit was conducted using the obtained wavenumber values as fixed parameters. An example of the profile analysis is given in Fig. 3.A, C, E. From these fits we have obtained the calibration curve by plotting the concentration of each molecule *vs.* the normalized integrated intensities (A/A_{1037}). As shown in Fig. 3.B, D, F, a linear dependence was obtained from the measurements, following the equation $c = ax + b$, where *c* is concentration of the solution in mol/L, *x* is the normalized integrated intensity A/A_{1037}, *a* is the slope defined as $F_{calibrant} \cdot C_{calibrant}/F$ and *b* is a constant close to zero (see Table 1).

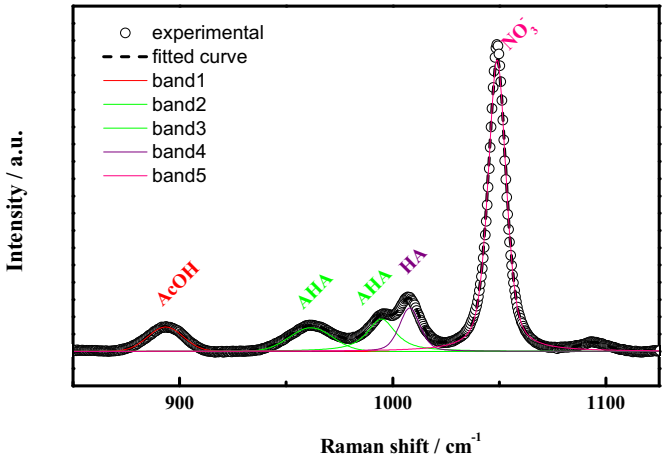

Fig. 4. Experimental and obtained fitted curves of the Raman spectra corresponding to 1 mol/L AHA solution after 5 h of hydrolysis in 0.5 mol/L HNO_3.

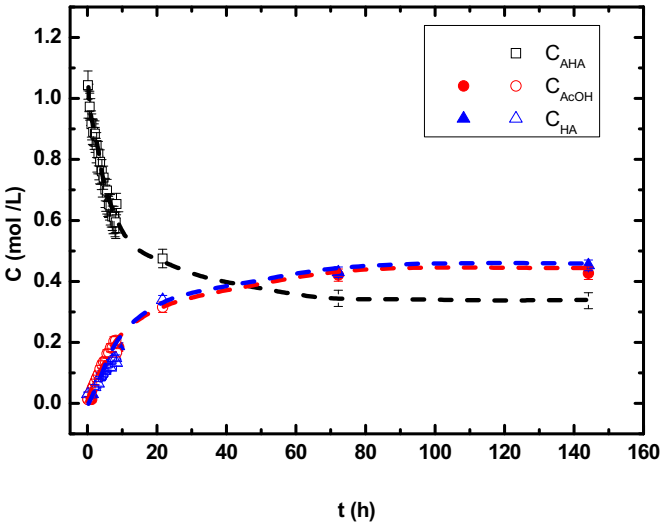

Fig. 5. Evolution of the concentrations of AHA, AcOH and HA as a function of time (from 0 to 150 h) in 0.5 mol/L HNO_3. (Open and solid symbols indicate results obtained from different experiments performed at the same conditions, see Section 2 for details).

By using these relations the concentration of AHA, AcOH and HA can be obtained from the analysis of each spectrum as a function of time. As an example, the experimental and the obtained fitted Raman spectra of AHA solution after 5 h of hydrolysis are shown in Fig. 4.

The results of the quantitative Raman analysis are shown in Fig. 5. As can be observed, AHA concentration decreases fast from 1 mol/L to ~0.30 mol/L, while AcOH and HA concentrations increase with time from 0 mol/L to ~0.40 mol/L, reaching the *plateau* after 20 h.

3.3. Comparison of techniques in rate constant calculations

Many authors calculate the rate constant of the AHA hydrolysis by indirect colorimetric techniques. In this section these results have been compared with the ones obtained by direct QRS.

In the literature, the reaction that occurs as a result of hydrolysis is considered to follow pseudo-first order kinetics with respect to AHA [10,14], as follows:

$$-\frac{d\,[AHA]}{dt} = k[AHA][H^+] \quad (5)$$

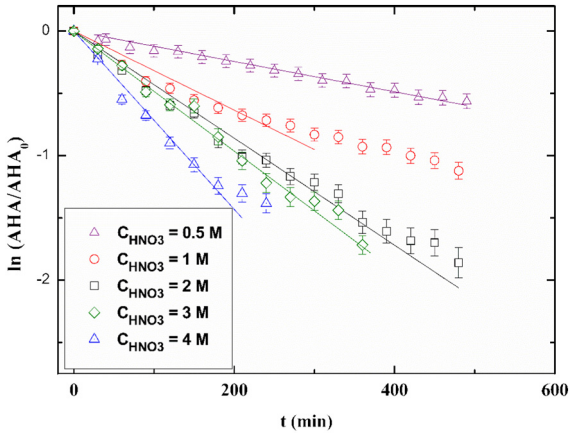

Fig. 6. Ln [AHA/AHA_0] as a function of time and nitric acid concentration (initial AHA concentration of 1 mol/L in 0.5, 1, 2, 3 and 4 mol/L HNO_3 solutions).

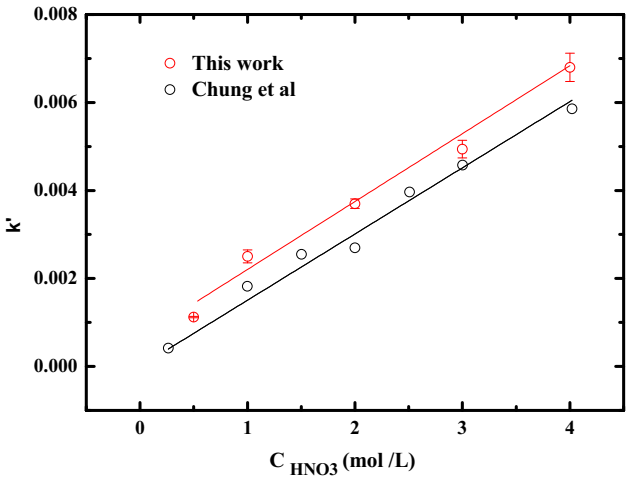

Fig. 7. Pseudo rate constant, k', as a function of acidic concentration at 25 °C. For the sake of comparison data from ref. [10] are also included.

$$-\frac{d\,[AHA]}{dt} = k\ddot{E}[AHA] \quad (6)$$

where k means the rate constant and k' is the apparent rate constant, which depends on the acid concentration as

$$k\ddot{E} = k\,[H^+]. \quad (7)$$

Therefore, several studies have determined that the dependency of $\ln[AHA/AHA_0]$ on time is a linear function of slope k' at a constant acid concentration, (Eq. (7)) for both excess conditions, as well as limiting nitric acid conditions, [7,8,10,11,14,29]. It is important to mention that since one of the products of this reaction, HA, consumes protons as it is being formed to give rise to NH_3OHNO_3, linear dependence of k' is only expected at the early beginning of the reaction.

Following the same analysis, Fig. 6 shows the $\ln[AHA/AHA_0]$ as a function of time (Eq. (3)) of an initial concentration of 1 mol/L AHA in HNO_3 solution of 0.5, 1, 2, 3 and 4 mol/L obtained by the *in situ* QRS analysis. These results show a linear function of slope k' and the hydrolysis rate increases with the acid nitric concentration up to 4 mol/L.

In order to determine the hydrolysis rate constant, Fig. 7 shows the dependence of k' as a function of acidic concentration. The change in k' *vs.* HNO_3 concentration yields a straight behavior of slope k for the HNO_3 studied concentrations (up to 4 mol/L).

Several published studies [8,11] consider the validity of this straight behavior only up to 3 mol/L HNO_3. However, it is important to highlight that the behavior found in this work, in which the apparent rate constant k' *vs.* HNO_3 at concentration up to 4 mol/L yields a straight behavior of slope k, is in good agreement with the data reported by Chung and Lee [10]. That means these kinetics equations could still be appropriate for describing other extraction systems typically used in the recycling of spent nuclear fuel. From Eq. (4) we have obtained a k value of 0.00152 ± 0.00001 L mol^{-1} min^{-1}.

The rate constant k at 25 °C for the hydrolysis of AHA has been determined by several authors (see Table 2) finding no appreciable differences in the reported values.

The k value obtained in this work is in perfect agreement with those obtained by Chung and Lee [10] and Sampath et al. [14], but different to the ones reported by Taylor and May [7], Carrott et al. [8] and Alyapyshev et al. [30]. One of the other typical restrictions for Eq. (3) is also to fit $[HNO_3] > [AHA]$ relation. Therefore, as k is independent of nitric acid concentration, for a better comparison, Table 2 shows the relation of nitric acid and AHA concentration. However, no clear reported correlation between differences in k values has been found, which may point out to a sum of factors, including time chosen for fitting or measurement conditions. Colorimetric conditions used for measurements have also been collected in Table 2 (last column) in order to highlight the different complexes AHA-Fe studied as a function of the different conditions such as AHA:Fe ratio, pH and concentrations.

4. Conclusions

In this work, the kinetics of acetohydroxamic acid hydrolysis in nitric acid solution was studied for the first time by a Quantitative Raman spectroscopy (QRS). The QRS has been developed as a direct and very accurate method to study the evolution of AHA hydrolysis as an alternative to traditional indirect UV–Vis methods.

Raman spectroscopy technique is an effective, faster and easier tool for determining the AHA hydrolysis in acidic media, since it can be used for *in situ* measurements, depending neither on the AHA-Fe complex formed nor on pH or concentrations. In addition, it allows us not only to monitor the decrease of AHA concentration, like UV–Vis method, but also the concentration increase of the hydrolysis products, AcOH and HA. QRS enables likewise a greater versatility in AHA complexation experiments due to the fact that no additive needs to be added to the system for measurements.

Many authors have reported AHA hydrolysis studies by using traditional indirect UV–Vis method, nonetheless the obtained rate constant data k are not in agreement, *i.e.* k varies from 0.0009 to 0.0021 L mol^{-1} min^{-1}. In this study, the value of rate constant k at 25 °C was estimated from experimental results and reported as 0.00154 ± 0.00001 L mol^{-1} min^{-1} not only for excess but also for non-excess conditions of nitric acid. It should be noted that apparent rate constant k' *vs.* HNO_3 concentration up to 4 mol/ L yields a straight behavior of slope k, in contrast with the theoretical studies, which predict a validity of this straight behavior only up to 3 mol/L HNO_3.

Table 2
Rate constants of the hydrolysis reactions, k, obtained at different conditions (*i.e.* excess conditions and limiting nitric acid conditions ($[HNO_3] < [AHA]$ and $[HNO_3] > [AHA]$), for different authors by using colorimetric methods compared with the one obtained in this work by QRS.

k ($L\ mol^{-1}\ min^{-1}$)	*Authors*	*Conditions*	*Method*
0.00205	Taylor and May 1999 [7]	$[HNO_3] > [AHA]$	Colorimetric λ_{max} = 499 nm
0.0015	Chung and Lee 2006 [10]	$[HNO_3] > [AHA]$	Colorimetric λmax = 503 nm
0.0009*	Alyapyshev et al. 2007 [30]	$[HNO_3] > [AHA]$	Colorimetric λmax = 498 nm
0.00184	Andrieux et al. 2007 [11]	$[HNO_3] > [AHA]$	Colorimetric λmax = 500 nm
0.00211	Carrot et al. 2008 [8]	$[HNO_3] > [AHA]$	Colorimetric λmax = 499 nm
0.0014	Sampath et al. 2011 [14]	$[HNO_3] < [AHA]$ and $[HNO_3] > [AHA]$	Colorimetric λmax = 500 nm
0.00152	This work	$[HNO_3] < [AHA]$ and $[HNO_3] > [AHA]$	QRS

* Calculated in this work from the published $k' = 0.00152, 0.00181, 0.00240$ at 1.5, 2, and 2.5 mol/L of HNO_3, respectively.

CRediT author statement

Iván Sánchez-García, Investigation
Laura J. Bonales, Supervision, Methodology, Formal analysis, Investigation, Writing - Original Draft
Hitos Galán, Validation, Conceptualization
Jose Manuel Perlado Funding acquisition
Joaquín Cobos Funding acquisition

Declaration of competing interests

The authors declare that they have no known competing financial interests or personal relationships that could have appeared to influence the work reported in this paper.

Acknowledgments

This work has been developed under the framework of CIEMAT-ENRESA collaboration agreement (Estudio y evaluación de la sostenibilidad de los procesos de separación hidrometalúrgica de radionucleidos de vida larga, SOPSEP project, ref. no 0079000269).

References

[1] S.P. Gupta, Hydroxamic Acids: A Unique Family of Chemicals with Multiple Biological Activities, Springer, 2013.
[2] Y.S. Fedorov, B.Y. Zilberman, A. Kopyrin, S. Arkhipov, Radiochemistry 43 (2001) 166–171.
[3] W. Lanham, T. Runion, PUREX Process for Plutonium and Uranium Recovery, Oak Ridge National Lab, Tenn, 1949.
[4] G.F. Vandegrift, M.C. Regalbuto, S. Aase, H. Arafat, A. Bakel, D. Bowers, J.P. Byrnes, M.A. Clark, J.W. Emery, J.R. Falkenberg, Waste Manag. 4 (2004) 1–22.
[5] J.A. Mitchell, R.M. Counce, J. Watson, B.B. Spencer, G.D. Del Cul, Nucl. Technol. 165 (2009) 360–369.
[6] R. Taylor, I. May, A. Wallwork, I. Denniss, N. Hill, B.Y. Galkin, B.Y. Zilberman, Y.S. Fedorov, J. Alloys Compd. 271 (1998) 534–537.
[7] R. Taylor, I. May, Czechoslov. J. Phys. 49 (1999) 617–621.
[8] M. Carrott, O. Fox, G. LeGurun, C. Jones, C. Mason, R.J. Taylor, F. Andrieux, C. Boxall, Radiochim. Acta 96 (2008) 333–343.
[9] K. Ghosh, Industrial & Engineering Chemistry 36B (1997) 1089–1102.
[10] D.Y. Chung, E.H. Lee, J. Ind. Eng. Chem. 12 (2006) 962–966.
[11] F.P.L. Andrieux, C. Boxall, R. Taylor, J. Solut. Chem. 36 (2007) 1201–1217.
[12] F.P.L. Andrieux, C. Boxall, I. May, R. Taylor, J. Solut. Chem. 37 (2008) 215–232.
[13] F.P. Andrieux, C. Boxall, H.M. Steele, R.J. Taylor, J. Solut. Chem. 43 (2014) 608–622.
[14] M. Sampath, P. Sinha, S. Kumar, U. Mudali, R. Natarajan, J. Radioanal. Nucl. Chem. 291 (2011) 649–651.
[15] S. Edwards, F. Andrieux, C. Boxall, M. Sarsfield, R. Taylor, D. Woodhead, Dalton Trans. 48 (2019) 673–687.
[16] B. Wopenka, J.D. Pasteris, Anal. Chem. 59 (1987) 2165–2170.
[17] L. J. Bonales, I. S. Garcia and J. Cobos, *Manuscript in progress*.
[18] J. Coates, Encyclopedia of Analytical Chemistry: Applications, Theory and Instrumentation, 2006.
[19] G. Walrafen, M. Fisher, M. Hokmabadi, W.H. Yang, J. Chem. Phys. 85 (1986) 6970–6982.
[20] M. Xu, J.P. Larentzos, M. Roshdy, L.J. Criscenti, H.C. Allen, Phys. Chem. Chem. Phys. 10 (2008) 4793–4801.
[21] M.R. Waterland, D. Stockwell, A.M. Kelley, J. Chem. Phys. 114 (2001) 6249–6258.
[22] N.J. Mendoza, L.J.n. Bonales, V.G. Baonza, M. Cáceres, J. Phys. Chem. B 118 (2014) 9919–9925.
[23] R.S. Krishnan, K. Balasubramanian, Proceedings of the National Academy of Sciences, India Section B 59 (1964) 285–291.
[24] R. Nightingale, E. Wagner, J. Chem. Phys. 22 (1954) 203–208.
[25] M. Haurie, A. Novak, Spectrochim. Acta 21 (1965) 1217–1228.
[26] B.A. Holmén, M.I. Tejedor-Tejedor, W.H. Casey, Langmuir 13 (1997) 2197–2206.
[27] D.C. Edwards, S.B. Nielsen, A.A. Jarzęcki, T.G. Spiro, S.C. Myneni, Geochim. Cosmochim. Acta 69 (2005) 3237–3248.
[28] A. Nevin, I. Osticioli, D. Anglos, A. Burnstock, S. Cather, E. Castellucci, Anal. Chem. 79 (2007) 6143–6151.
[29] S.N. White, Appl. Spectrosc. 64 (2010) 819–827.
[30] M. Alyapyshev, A. Paulenova, M.A. Cleveland, J.E. Bruso, P. Tkac, GLOBAL Conference, Boise, Idaho, 2007.